

Interband mixing between two-dimensional states localized in a surface quantum well and heavy hole states of the valence band in narrow gap semiconductor

V.A.Larionova and A.V.Germanenko

Institute of Physics and Applied Mathematics,

Ural University, Ekaterinburg 620083, Russia

(August 13, 2018)

Abstract

Theoretical calculations in the framework of Kane model have been carried out in order to elucidate the role of interband mixing in forming the energy spectrum of two-dimensional carriers, localized in a surface quantum well in narrow gap semiconductor. Of interest was the mixing between the 2D states and heavy hole states in the volume of semiconductor. It has been shown that the interband mixing results in two effects: the broadening of 2D energy levels and their shift, which are mostly pronounced for semiconductors with high doping level. The interband mixing has been found to influence mostly the effective mass of 2D carriers for large their concentration, whereas it slightly changes the subband distribution in a wide concentration range.

PACS number(s): 73.20.At, 73.40.Qv, 73.40.Gk

Typeset using REVTeX

I. INTRODUCTION

Interband mixing effects attract much interest because they can play a decisive part in forming the energy spectrum of low-dimensional systems. Such is in the case for InAs-GaSb semimetallic superlattices, whose physical properties are determined by the mixing between valence band states of GaSb and conduction band states of InAs at the interfaces. [1–3]

Analogous situation takes place in a metal–insulator–semiconductor structure based on a narrow gap semiconductor. [4–9] A small value of the energy gap in the semiconductor leads to the fact that at energies below the top of the valence band the two-dimensional (2D) states localized in a surface quantum well can mix with the valence band states and 2D carriers can tunnel from the space charge region into the valence band states in the volume of semiconductor. This results in a shift of the 2D subband energies and a broadening of these levels. [4–7] Due to high value of the effective mass, the probability of tunneling of 2D carriers into the heavy hole states is small. Therefore the interband mixing with the heavy hole states was neglected. This approach is justified for semiconductors with low impurity density, because the surface potential in such materials is smooth in the shape, and the 2D states localized in the quantum well are spatially separated from the valence band by a wide region of forbidden energies.

In semiconductors with high doping level the effects of interband tunneling of 2D electrons into the heavy hole states can be stronger. The influence of these effects on the energy spectrum and broadening of the 2D states localized in the surface quantum well in the narrow gap semiconductor (HgCd)Te is discussed in the present article.

II. THEORETICAL MODEL

A small value of the energy gap (E_g) in semiconductor investigated makes it necessary to employ a multiband Hamiltonian in the kP -based calculations of the energy spectrum. We started from the multiband Hamiltonian derived from Kane’s model making the usual

assumption that the energy difference between the valence Γ_8 -band and spin-orbit split-off Γ_7 -band is infinite. To consider the effects involving the heavy hole states, the interaction with remote bands has been taken into account by a standard procedure of including additional terms with γ -parameters in the Hamiltonian. [10] An isotropic approximation has been used.

The Kane Hamiltonian, which is a 6×6 matrix in the above assumptions, can be block diagonalized, when the axis z is chosen to be normal to the interface and the axis y along the direction of the carrier motion. In this case the Hamiltonian is two 3×3 matrices for two groups of states. One of the matrices is defined by

$$\hat{H}^+ = \begin{pmatrix} E^{\Gamma_6}(z) & i\sqrt{\frac{2}{3}}P\left(\frac{k}{2} - \frac{\partial}{\partial z}\right) & \frac{i}{\sqrt{2}}Pk \\ i\sqrt{\frac{2}{3}}P\left(-\frac{k}{2} - \frac{\partial}{\partial z}\right) & \mathcal{G} & -\sqrt{3}\frac{\hbar^2}{2m_0}\gamma\left(k^2 + 2k\frac{\partial}{\partial z}\right) \\ -\frac{i}{\sqrt{2}}Pk & -\sqrt{3}\frac{\hbar^2}{2m_0}\gamma\left(k^2 - 2k\frac{\partial}{\partial z}\right) & \mathcal{F} \end{pmatrix}, \quad (1)$$

$$\mathcal{G} = E^{\Gamma_8}(z) + \frac{\hbar^2}{2m_0} \left((\gamma_1 + 2\gamma) \frac{\partial^2}{\partial z^2} - (\gamma_1 - \gamma) k^2 \right) + e\varphi(z),$$

$$\mathcal{F} = E^{\Gamma_8}(z) + \frac{\hbar^2}{2m_0} \left((\gamma_1 - 2\gamma) \frac{\partial^2}{\partial z^2} - (\gamma_1 + \gamma) k^2 \right) + e\varphi(z),$$

where $k \equiv k_y$, P is the momentum matrix element, γ_1, γ are the parameters, which describe the interaction with remote bands, $\varphi(z)$ is the electrostatic potential, and $E^{\Gamma_6}(z)$, $E^{\Gamma_8}(z)$ are the energies of the conduction and valence band edges, respectively. Here, the assumption has been made that the values of P , γ_1 , and γ are independent of coordinate.

The second matrix H^- is obtained from H^+ by replacing k by $-k$.

The electrostatic potential can be derived from the Poisson equation. We assumed $\varphi(z)$ to be parabolic in the space charge region and constant in the volume of semiconductor:

$$\varphi(z) = \begin{cases} \varphi_s(1 - z/L)^2, & 0 \leq z \leq L \\ 0, & z > L, \end{cases} \quad (2)$$

where

$$\varphi_s = \varphi(0), \quad L = \left(\frac{2\kappa\kappa_0\varphi_s}{e(N_A - N_D)} \right)^{1/2}.$$

Here, $N_A - N_D$, and κ stand for density of acceptors uncompensated, and dielectric constant, respectively. Expression (2) is a good approximation for the case when the concentration of 2D electrons is less than the value of $(N_A - N_D)L$.

Thus, Schrödinger equation is two independent systems of differential equations of the second order. For solving these systems boundary conditions have to be deduced. The introduction of the boundary conditions is based on a model proposed in Refs. [4] and [11] for calculation of the energy spectrum of 2D states in MIS structures, based on ordinary and inverted semiconductors, respectively. As in these papers, we supposed (see Fig.1a): (i) the band structure of insulator to be identical to that of semiconductor; (ii) the energy gap in the insulator to be much greater than that in semiconductor, and the conduction and valence band offsets, denoted as D_c and D_v , respectively, to exceed the value of E_g ; (iii) the energy bands in the insulator to be “flat”, i.e. $\varphi(z < -d) = \text{const}$, and (iv) the structure to have a smooth insulator/semiconductor interface of width d with linear dependence of the band-edge energies on z coordinate. [11]

Since a general solution of the Kane Hamiltonian for $\varphi(z) = \text{const}$ is known, the wave function on the insulator ($z < -d$) and semiconductor ($z > L$) sides of the structure can be simply derived.

For $z < -d$ it contains only the terms exponentially vanishing deep into the insulator. To choose the boundary conditions on the semiconductor side let us briefly consider three different cases, which can be realized depending on the energy and longitudinal component of quasimomentum of 2D state. First, the 2D state is not degenerate with the valence band (region I in Fig.1b). In this case the wave function exponentially diminishes deep into the volume of semiconductor. Second, the 2D state is degenerate only with the heavy hole valence band (region II). In this case the normal component of the light hole quasimomentum is imaginary. Therefore, the wave function in this case is a superposition of the light hole term, which diminishes exponentially deep into the semiconductor, and two oscillating

terms presenting the plane wave associated with the heavy hole. Third, the 2D state is in resonance with both heavy and light hole valence bands (region III) and the wave function is a superposition of two plane waves corresponding to the light and heavy holes. In the present paper we focus our attention on the second case.

Thus, starting from the exact solution of the Kane Hamiltonian on the insulator side we numerically integrated the differential equation systems through the space charge region and chose those solutions which satisfy the boundary conditions on the semiconductor side.

It is clear that in region II the eigenvalue problem has a continuous spectrum of solutions, i.e. at any energy value we can find the wave function satisfying the boundary conditions. To define the energy level associated with the resonant 2D states and its broadening caused by the interband mixing between the 2D states and heavy hole states, the Levinson's theorem has been applied. [4,7]

III. DISCUSSION

To analyze peculiarities of the energy spectrum of 2D states arising from the interband mixing, we have performed numerical calculations using realistic parameters which are close to the parameters of the sample investigated in Ref. [14]. They are the following: $E_g = 50$ meV, $N_A - N_D = 6 \times 10^{17} \text{ cm}^{-3}$, $\kappa = 20$. The calculations have been carried out using two sets of γ -parameters: $\gamma_1 = 2.0$, $\gamma = 0$ (Ref. [11]) and $\gamma_1 = 4.5$, $\gamma = 1.0$ (Ref. [12]). To make identical the dispersion law of bulk electron states calculated with different sets of γ -parameters, we changed slightly the value of the momentum matrix element P from $8.0 \times 10^{-8} \text{ eV}\cdot\text{cm}$, for the first set, to $8.1 \times 10^{-8} \text{ eV}\cdot\text{cm}$, for the second one. Parameters of the insulator/semiconductor interface are the same as in Ref. [11]: $D_c = 2 \text{ eV}$, $D_v = 1 \text{ eV}$, and $d = 10 \text{ \AA}$.

Figure 2 shows the energy spectrum of 2D states calculated with different sets of γ -parameters as compared with the energy spectrum of 2D states calculated in the infinite heavy hole mass approximation with a so-called "mid-gap" boundary condition on the semi-

conductor side. [13] Two branches of the energy spectrum specified by k^+ and k^- are the results of calculation for two groups of states. These branches are two “spin” branches of the ground 2D subband split by spin-orbit interaction in an asymmetric quantum well. [14–18] It is clearly seen from the figure that the interband mixing of 2D states with the heavy hole states results in the energy shift of 2D subbands. The smaller is the heavy hole effective mass ($m_h = m_0/(\gamma_1 - 2\gamma)$) the lower is the energy position of the 2D subbands.

One more important feature of the energy spectrum of 2D states appearing due to interband mixing is the broadening of 2D energy levels. This broadening is shown in Fig.2 as hatched region. As is seen the broadening of 2D levels is negligibly small for energies close to the top of the valence band in the volume of semiconductor. At more negative energies both 2D “spin” sublevels become broad. The value of broadening is different for k^+ and k^- sublevels for a fixed energy. It increases with decreasing energy or quasimomentum value. The maximum value of the broadening is about 10 meV. It is comparable to the broadening of 2D states appearing due to tunneling into the light hole states which has been calculated in Ref. [5] for a sample with close parameters. On further decreasing quasimomentum the 2D states fall in resonance with the light hole valence band (region III in Fig. 1b). Note that the broadening value slightly depends on the heavy hole effective mass.

Thus, the interband mixing between the 2D states and heavy hole states leads to two effects: the shift of subband energies and the broadening of 2D levels. Let us consider how these effects can manifest themselves in experiment.

Traditional experimental methods, such as galvanomagnetic investigations, volt-capacitance spectroscopy, give information about the carriers at the Fermi energy. In p -type (HgCd)Te the Fermi level lies near the top of the valence band in the energy range $-5\dots+5$ meV at low temperatures. As was shown above for these energies the broadening of 2D states is small and therefore these methods must not be sensitive to this effect. Tunneling investigations allow to get information about the 2D states in a wide energy range including the energies, where the broadening is large. Besides, the maximum value of broadening is comparable with the cyclotron energy in magnetic fields right up to 2 T. This can result

in additional broadening of resonance peaks in magneto-optical and cyclotron resonance experiments.

As to the effect connected with the influence of interband mixing on the dispersion law of 2D states traditional experimental methods give no way of direct deducing a quasimomentum dependence of the energy of 2D states for a fixed value of a surface quantum well. For example, in tunneling experiments [11,19] a voltage bias, applied to the structure, changes not only the energy tested, but surface potential as well. The value of the surface potential is usually used as a fitting parameter in analyzing experimental data, for example, dependences of 2D subband concentration and the effective mass of 2D carriers on their total concentration. Figure 3 shows the relationship between 2D subband concentration and the total concentration of 2D electrons, calculated using two sets of γ -parameters and infinite heavy hole effective mass. The concentration of 2D electrons is changed by varying the surface quantum well depth from 250 to 320 mV. It is clearly seen from the figure that the interband mixing does not cause essential changes in the subband distribution of 2D electrons. One can see only slight increase in ratio between concentrations of 2D electrons in k^+ and k^- “spin” subbands with decreasing the heavy hole effective mass. Thus, in spite of the fact that the interband mixing results in shifting the energy positions of 2D subbands, it does not strongly influence the subband distribution of 2D electrons.

The effective mass of carriers is a differential characteristic of the energy spectrum and it might be more sensitive to the interband mixing effects. We have calculated the effective mass of 2D electrons $m^* = \hbar^2 k (\partial E / \partial k)^{-1}$ at $E = E_F$ as a function of their total concentration (Fig. 4). As is clearly seen for large concentration of 2D carriers ($N_S > 0.55 \times 10^{12} \text{cm}^{-2}$) the effective mass of 2D electrons, calculated in the model taking into account the interband mixing (solid and dashed curves), is larger than that calculated with the infinite heavy hole mass (dotted curves). The difference increases with increasing the total concentration of 2D electrons. It is evident that the concentration dependence of the effective mass, calculated with $\gamma_1 = 4.5$, $\gamma = 1.0$ deviates mostly from the results obtained in the infinite heavy hole mass approximation. For k^+ -“spin” states this difference is larger and at $N_S \simeq 10^{12} \text{cm}^{-2}$ it

comes to more than 10%.

A distinctive situation occurs for small concentrations of 2D electrons ($N_S < 0.45 \times 10^{12} \text{cm}^{-2}$) for k^+ -group of states. The effective mass, calculated with γ -parameters, monotonically decreases with decreasing the total concentration, whereas the effective mass, calculated in the framework of the infinite heavy hole mass approximation, goes through a minimum, and at some value of the total concentration it becomes larger than the effective mass calculated with γ -parameters. To explain this peculiarity, let us turn to Figure 2. One can see that the bottom of k^+ -subband lies at $k \neq 0$ (the dotted curve in the figure). As a consequence, the effective mass $m^* = \hbar^2 k (\partial E / \partial k)^{-1}$ turns to infinity on the bottom and is sufficiently large in its vicinity. For the low concentrations of 2D electrons, this portion of the energy spectrum is found to be near the Fermi level for the case of infinite heavy hole mass, whereas it is lower in the energy when the finite value of the heavy hole mass is taken into account. This reflects in the behavior of the effective mass of 2D carriers for their low concentration.

Thus, the presented results show that the interband mixing causes the effective mass of 2D states to be larger than that calculated in the infinite heavy hole mass approximation. This is more evident for k^+ -“spin” states and for large concentration of 2D carriers. The effective mass of 2D carriers calculated with the most-used set of γ -parameters [12] differs mostly from the results of calculation, in which the interaction with remote bands is neglected. To our knowledge there are no experimental data concerning the effective mass of 2D states in highly doped narrow gap semiconductors in case, when 2D states are in resonance with the heavy hole valence band.

IV. CONCLUSION

The effects of interband mixing between 2D states and heavy hole valence band states are found to influence the energy spectrum of 2D states localized in a surface quantum well in the narrow gap semiconductor with high doping level. They manifest themselves in

the broadening of 2D energy levels, which is sufficiently large for the energies close to the bottom of 2D subband, and the shift of 2D subbands to lower energies. The latter does not practically affect the concentration dependence of subband distribution of 2D carriers, but leads to a change of their effective mass for high total concentrations of 2D carriers.

REFERENCES

- [1] M. Altarelli, Phys. Rev. B **28**, 842 (1983).
- [2] A. Fasselino and M. Altarelli, Surf. Sci. **142**, 322 (1984).
- [3] H. Sakaki, L.L. Chang, G.A. Sai-Halasz, C.A. Chang, and L. Esaki, Solid State Commun. **26**, 589 (1978).
- [4] Pawel Sobkowicz, Semicond. Sci. Technol. **5**, 183 (1990).
- [5] I. Nachev, Nuovo Cimento **12 D**, 1143 (1990).
- [6] A. Ziegler and U. Rössler, Europhys. Lett. **8**, 543 (1989).
- [7] B. Freytag, U. Rössler, and O. Pankratov, Semicond. Sci. Technol. **8**, S243 (1993).
- [8] U. Kunze, Z. Phys. B – Condensed Matter **80**, 47 (1990).
- [9] J. Müller and U. Kunze, Semicond. Sci. Technol. **8**, 703 (1990).
- [10] G.L. Bir and G.E. Pikus, *Symmetry and Strain Induced Effects in Semiconductors* (Wiley, New York, 1974).
- [11] G. M. Minkov, A. V. Germanenko, V. A. Larionova, and O. E. Rut, Phys. Rev. B **54**, 1841 (1996).
- [12] Y. Guldner, C. Rigaux, A. Mycielski, and Y. Couder, Phys. Stat. Sol. b **82**, 149 (1977).
- [13] G.E. Marques and L.J. Sham, Surf. Sci. **113**, 131 (1982).
- [14] G. M. Minkov, O. E. Rut, and A. V. Germanenko, (unpublished).
- [15] Y.A. Bychkov and E.I. Rashba, J. Phys. C **17**, 6039 (1984).
- [16] F.J. Ohkawa and Y. Uemura, J. Phys. Soc. Jpn. **37**, 1325 (1974).
- [17] R. Wollrab, R. Sizmann, F. Koch, J. Ziegler, and H. Maier, Semicond. Sci. Technol. **4**, 491 (1989).

[18] R.Sizmann and F.Koch, *Semicond. Sci. Technol.* **5**, S115 (1990).

[19] G. M. Minkov, O. E. Rut, V. A. Larionova, and A. V. Germanenko, *Zh. Éksp. Teor. Fiz.* **105**, 719 (1994) [*JETP* **78**, 384 (1994)].

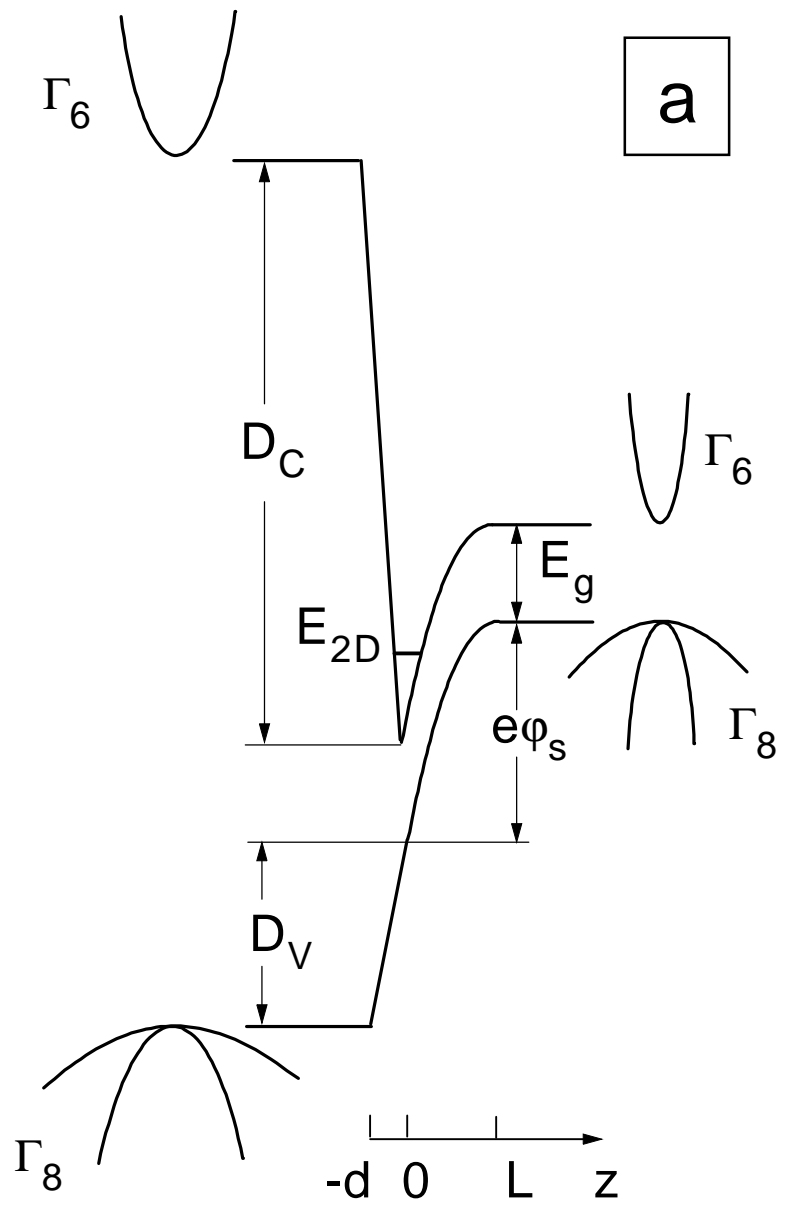
FIGURES

FIG. 1. (a) Model of an insulator – narrow gap semiconductor structure with a surface quantum well used in the calculations. (b) The dispersion law $E(k, k_z = 0)$ for carriers in the volume of semiconductors (solid curves). The hatched regions show the continuous spectrum. The numbers I, II, and III denote three different regions of the energy spectrum of 2D states (for details, see text)

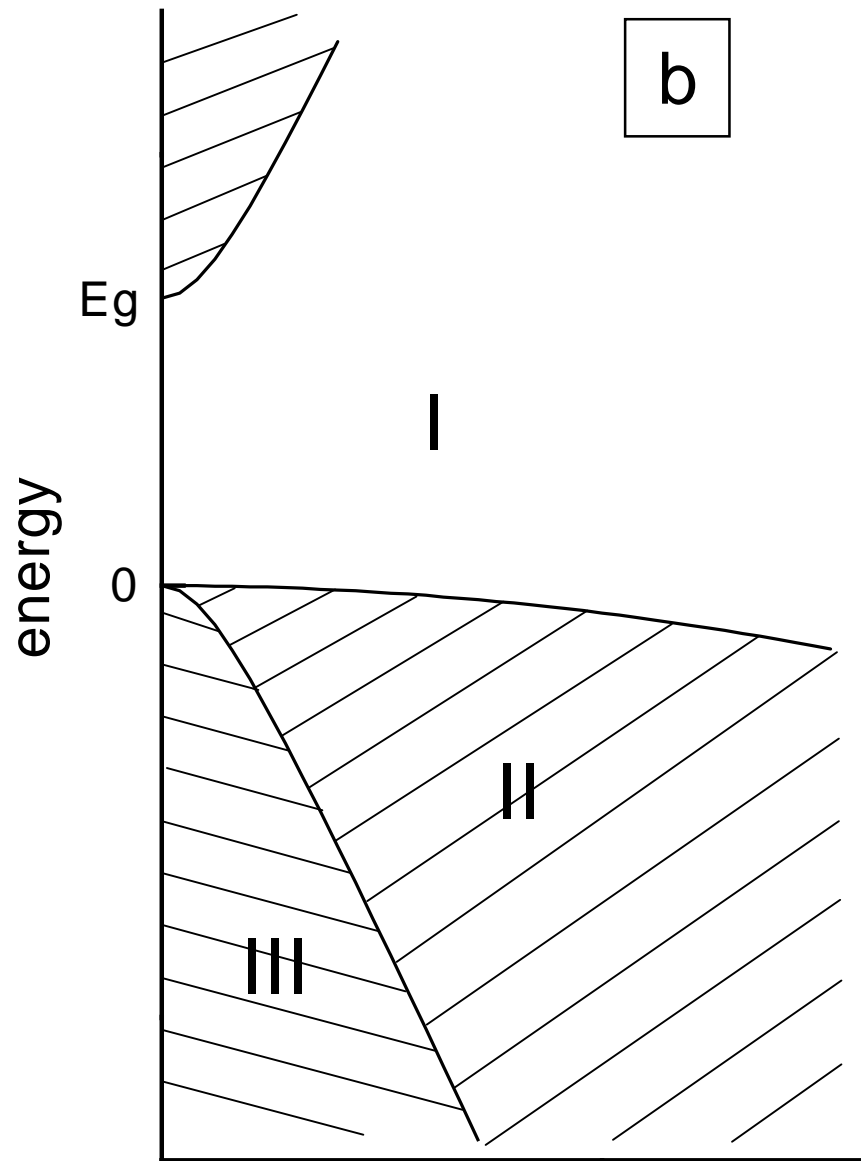
FIG. 2. The energy spectrum of 2D states calculated with different sets of γ -parameters: $\gamma_1 = 4.5$, $\gamma = 1.0$ (the solid curves) and $\gamma_1 = 2.0$, $\gamma = 0$ (the dashed curves), as compared with the energy spectrum of 2D states calculated in the infinite heavy hole mass approximation (the dotted curves). The value of the surface potential used in the calculations is 285 mV. k^+ and k^- denote two different “spin” branches of the energy spectrum. The dot-dash curves show the borders of region II, where the 2D states are in resonance with the heavy hole valence band.

FIG. 3. The dependence of the electron concentration in each 2D subband on the total concentration of 2D electrons. The notations and curve types are the same as in Fig. 2.

FIG. 4. The dependence of the electron effective mass on the total concentration of 2D electrons. The notations and curve types are the same as in Fig. 2.



Insulator Semiconductor



quasimomentum

